

THE DUSTY ENVELOPES OF FU ORIONIS VARIABLES¹

SCOTT J. KENYON^{2,3} AND LEE W. HARTMANN²

Harvard-Smithsonian Center for Astrophysics, 60 Garden St., Cambridge, MA 01238

Received 1991 April 15; accepted 1991 June 25

ABSTRACT

We discuss the spectral energy distributions of FU Orionis variables, using new ground-based infrared photometry and *IRAS* ADDSCAN measurements. Nearly half of the recognized FU Orionis variables are heavily extinguished, so further analysis is difficult. Three (V1057 Cyg, V1515 Cyg, Z CMa) of the remaining five objects have much larger far-infrared fluxes than can be explained by the simple accretion disk models that match their spectral energy distributions for $\lambda < 10 \mu\text{m}$. The 10–20 μm excess emission in V1057 Cyg has decreased proportionately with the decline in optical light, which demonstrates that the far-infrared flux arises in a dust shell reprocessing light from the central object. The amount of dust required to explain the far-infrared excess emission of V1057 Cyg is much larger than that implied by the optical extinction, so the dust distribution is not spherically symmetric.

In principle, a geometrically flared disk can account for the far-infrared emission, but in practice the large solid angle the disk must subtend at the star appears difficult to achieve in a reasonable physical model. We suggest instead that the far-infrared excesses arise in somewhat flattened dusty envelopes with a covering factor in solid angle of roughly $\frac{1}{2}$, which is consistent with the fraction of FU Orionis variables that are heavily embedded. The dusty envelope in V1057 Cyg must have an inner radius of ~ 10 AU to explain the excess emission at 10 μm , and this envelope probably cannot be static so close to the central star. We propose that the dusty envelope falls onto the outer disk at a rate of $\sim 5 \times 10^{-6} M_{\odot} \text{yr}^{-1}$. This rate is sufficient to replenish disk material accreted during a FU Orionis outburst and allow repetitive eruptions on time scales of several thousand years.

Subject headings: interstellar: grains — stars: circumstellar shells — stars: pre-main-sequence

1. INTRODUCTION

The FU Orionis variables are eruptive pre-main-sequence systems found in regions of star formation. Most members of this class—FU Ori, V1057 Cyg, V1515 Cyg, V1735 Cyg, and V346 Nor—have undergone 4–6 magnitude outbursts and have remained luminous for decades (Herbig 1977; Hartmann, Kenyon, & Hartigan 1991). The pre-main-sequence objects Z CMa, L1551 IRS 5, and BW 76 are also usually included in the FU Ori class. Large eruptions have not been identified in these objects, but their spectroscopic and photometric properties identify them as FU Orionis variables (Mundt et al. 1985; Carr, Harvey, & Lester 1987; Herbig 1989; Hartmann et al. 1989; Reipurth 1985, 1991; Eisloffel, Hessman, & Mundt 1990).

In previous papers, we have shown that rapid accretion through a circumstellar disk onto a T Tauri star quantitatively accounts for many remarkable properties of FU Orionis variables (Hartmann & Kenyon 1985, 1987a, b; Kenyon, Hartmann, & Hewett 1988, hereafter KHH). Specifically, quasi-steady accretion-disk models explain the broad spectral energy distributions, the variation of spectral type and rotational velocity with the wavelength of observation, and the

double-peaked nature of the absorption line profiles (Hartmann 1991; Hartmann & Kenyon 1991).

The steady accretion-disk model provides a good match to the observed spectral energy distributions of FU Ori, V1057 Cyg, and V1515 Cyg between 0.3 μm and 5 μm , but there is evidence for excess emission at wavelengths of 10–20 μm (see, for example, Simon & Joyce 1988) and 1–30 mm (Weintraub, Sandell, & Duncan 1989, 1991; Rodriguez, Hartmann, & Chavira 1991). Adams, Lada, & Shu (1987, hereafter ALS) suggested far-infrared emission in FU Ori might arise in the outer envelope of the parent molecular cloud core, and Simon et al. 1972 (see also Simon & Dyck 1977) proposed a circumstellar shell to account for 10–20 μm emission in V1057 Cyg. The observation of roughly symmetric reflection nebulae around these and other FU Orionis variables (see Goodrich 1987) similarly suggests the presence of remnant material from the original star-forming core.

This paper reports infrared (1–100 μm) observations of FU Orionis variables with a special emphasis on interpreting the decline of V1057 Cyg from optical maximum. We find that FU Orionis variables are typically surrounded by large amounts of dust, as many are heavily extinguished or have significant far-infrared excesses above the emission predicted by the steady-state accretion-disk model. We consider two possible dust envelope geometries to explain the far-infrared emission: a flared accretion disk reprocessing radiation emitted by disk material near the central star and an infalling remnant envelope of the molecular cloud core. The large covering factor required for the dust envelope of V1057 Cyg favors the infalling envelope model. This infalling gas, if it piles up in the disk, could provide the material for the large eruptions, in which

¹ Research reported herein used the Multiple Mirror Telescope, a joint facility of the Smithsonian Institution and the University of Arizona.

² Visiting Astronomer, Kitt Peak National Observatory, operated by the National Optical Astronomy Observatory under contract to the National Science Foundation.

³ Visiting Astronomer at the Infrared Telescope Facility, which is operated by the University of Hawaii under contract from the National Aeronautics and Space Administration.

TABLE 1
INFRARED PHOTOMETRY OF FU ORIONIS OBJECTS

Object	Julian Date	K	J-K	H-K	K-L	M	N	Q	Detector	Aperture
FU Ori	2,447,818.95	5.10	0.78	3.98	2.39	...	Bolo	5"
Z CMa	2,447,518.88	3.80	2.36	1.21	1.85	InSb	9"
	2,447,521.96	3.90	1.78	0.85	-1.25	...	Bolo	5"
V346 Nor	2,447,629.77	7.29	3.28	1.48	1.72	4.40	D2	6"
V1057 Cyg	2,447,797.78	5.78	1.58	0.66	1.07	RC2	6"
	2,447,797.85	4.01	1.61	-0.46	BOLO	6"
	2,447,798.74	5.79	1.53	0.64	1.07	RC2	6"
	2,447,798.80	3.99	1.57	-0.74	BOLO	6"
	2,447,798.81	1.58	-0.53	BOLO	6"
	2,447,816.61	5.83	0.99	3.86	1.49	...	Bolo	5"
	2,448,169.74	5.76	1.65	0.69	IRIM	10"
	2,448,178.67	5.78	1.64	0.68	IRIM	10"
	2,448,378.91	5.92	0.90	Bolo	5"
	2,448,379.91	5.82	0.90	...	1.50	...	Bolo	5"
	2,448,380.91	5.86	0.96	...	1.63	...	Bolo	5"
V1735 Cyg	2,446,718.72	6.55	2.74	1.04	HERMANN	12"
	2,447,519.56	6.66	2.88	1.16	1.06	InSb	9"
	2,447,521.55	6.64	2.83	1.13	1.06	InSb	9"
	2,447,797.79	6.69	2.72	1.09	1.14	RC2	6"
	2,447,797.89	4.95	3.61	1.54	BOLO	6"
	2,447,798.82	4.80	3.53	...	BOLO	6"
	2,447,799.80	3.58	...	BOLO	6"
	2,447,818.62	6.68	1.06	5.02	3.65	...	Bolo	5"
	2,448,169.79	6.68	2.93	1.17	InSb	9"
	2,448,175.71	6.69	2.83	1.14	IRIM	10"
	2,448,176.66	6.71	2.81	1.13	IRIM	10"
	2,448,178.68	6.71	2.83	1.13	IRIM	10"
	2,448,179.67	6.71	2.83	1.13	IRIM	10"

accretion rates rise to $\sim 10^{-4} M_{\odot} \text{ yr}^{-1}$ for periods of 10–100 yr.

2. OBSERVATIONS

2.1. New Photometry

Broad-band infrared (IR) photometry of several FU Ori variables has been obtained over the past few years with the HERMANN photometer on the 1.3 m telescope at Kitt Peak National Observatory, the RC2 and BOLO detectors at the 3 m Infrared Telescope Facility, and the InSb and Bolo detectors at the 4.5 m Multiple Mirror Telescope. The observations were made with standard chopping and beam-switching techniques and were reduced to the CIT photometric system using standard stars from Elias et al. (1982). Kenyon (1988) describes the reduction of KPNO photometry in more detail. Table 1 lists these data, which have uncertainties of $\pm 3\%$ at *JHK*, $\pm 4\text{--}5\%$ at *L* and *M*, $\pm 10\%$ at *N*, and $\pm 20\%$ at *Q*.

Additional near-IR photometry was acquired with the IR imager (IRIM) mounted on the 1.3 m telescope at Kitt Peak National Observatory. The data were recorded on a 62×58 InSb array which covered an area of roughly $1' \times 1'$. We took 15 frames with a standard *JHK* filter set—five per filter—and displaced the telescope by $8''$ in both right ascension and declination after each integration. Final object frames were produced by dividing the raw frames with an appropriate flat field and then subtracting a flattened sky frame. The flat field image was constructed by median filtering 6–10 sets of five 100 s integrations made through the night; the sky frame is the median-filtered image of the five object images obtained with each filter. We used the NOAO IRAF routines PHOT and QPHOT to perform photometry through a $10''$ aperture and reduced

these results to the Elias et al. (1982) system using standard techniques. The accuracy of the imager photometry is comparable to photometry with single channel detectors: $\pm 3\%$ at *JHK*.

FU Orionis variables are bright far-IR emitters, and all were detected by the *Infrared Astronomical Satellite (IRAS)* during its 1983 mission. Several objects did not appear in either version of the Point Source Catalog, but strong sources are present on ADDSCANS kindly provided by the *IRAS* Infrared Processing and Analysis Center. For completeness, we list ADDSCAN fluxes for all FU Orionis variables in Table 2.

2.2. Spectral Energy Distributions

We have collected published IR and optical photometry for eight FU Orionis variables and present their spectral energy distributions in Figures 1 and 2. V346 Nor, V1735 Cyg, and L1551 IRS 5 are too heavily extinguished to deredden their spectral energy distributions with any confidence. (A new FU

TABLE 2
IRAS ADDSCAN FLUXES FOR FU ORIONIS OBJECTS

Objects	IRAS				
	Designation	12 μm	25 μm	60 μm	100 μm
L1551 IRS 5	04284 + 1801	9.8	107.2	350.1	443.6
FU Ori	05426 + 0903	6.0	14.1	15.1	36.3
Z CMa	07013 - 1128	134.8	214.9	312.1	368.7
BBW 76	07486 - 3258	1.0	1.7	1.7	
V346 Nor	16289 - 4449	8.9	32.5	63.8	72.5
V1515 Cyg	20220 + 4202	4.0	8.0		
V1057 Cyg	20571 + 4403	14.9	30.4	54.7	26.0
V1735 Cyg	21454 + 4718	2.6	8.8	42.7	81.8

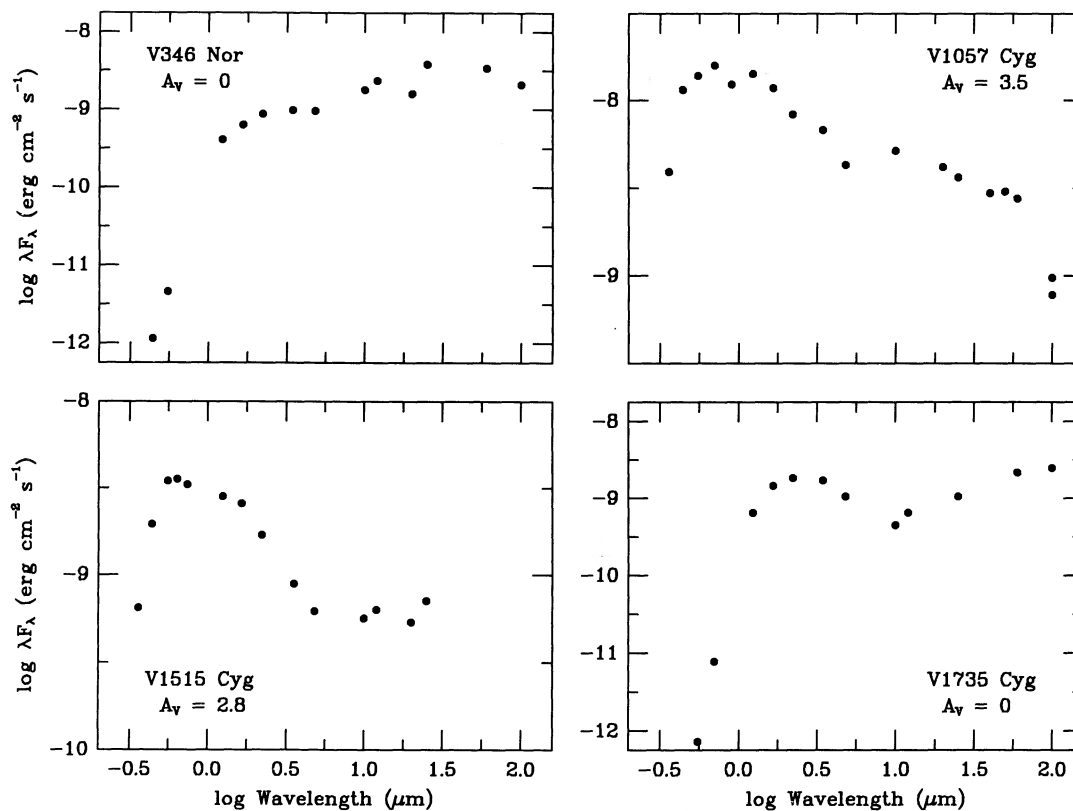


FIG. 1.—Spectral energy distributions for the FU Orionis objects V346 Nor (HH57 IRS), V1057 Cyg, V1515 Cyg, and V1735 Cyg (Elias 1-12). The data have been dereddened by the amounts shown in each panel. The fluxes have been compiled from Elias (1978; V1735 Cyg), Graham & Frogel (1985; V346 Nor), Kenyon, Hartmann, & Kolotilov (1991; V1515 Cyg), Kopatskaya (1984; V1057 Cyg), Shaimieva & Shutiomova (1985; V1057 Cyg), Simon & Joyce (1988; V1057 Cyg), and this paper.

Orionis variable candidate, RNO 1B, is similarly heavily embedded in dust [Staudé & Neckel 1991]. The other objects have been dereddened to produce optical colors consistent with their G-type spectral classifications, as described by Hartmann & Kenyon (1985). For Z CMa this process results in any extremely “flat” spectral energy distribution from 5000 Å to almost 100 μm. The remaining three objects all have a broad maximum in λF_λ centered roughly at 1 μm.

2.3. Spectral Evolution of V1057 Cyg

V1057 Cyg is the only FU Orionis variable with a well-documented decline from optical maximum. Figure 3 shows light curves at *B* (0.44 μm), *V* (0.55 μm), *K* (2.2 μm), *N* (10 μm), and *Q* (20 μm) using data from the literature and Table 1. The amplitude of the decline decreases monotonically from the ultraviolet to the mid-infrared and ranges from roughly 4 mag at *U* (0.36 μm) to about 0.5 mag at *M* (5 μm). The amplitude is larger at 10–20 μm than at 5 μm, as the system declined by ~1.5 mag at *N* and ~2–2.5 mag at *Q*.

3. MODELS FOR THE SPECTRAL ENERGY DISTRIBUTION OF V1057 CYG

Steady accretion-disk models explain the spectral energy distributions of V1057 Cyg and FU Ori shortward of $\lambda = 10$ μm (KHH). However, the observed radiation at far-IR wavelengths exceeds the prediction of a steady-state disk model. This far-IR excess is small in FU Ori but is approximately 25% of V1057 Cyg’s total luminosity. The excess probably is not caused by the large *IRAS* beam size, because the *IRAS* fluxes

typically agree with small beam measurements made from the ground (10–20 μm) and from the Kuiper Airborn Observatory (40–160 μm). Several authors (for example, Rieke, Lee, & Coyne 1972; Simon et al. 1972) have proposed a circumstellar dust shell for the far-IR emission; ALS and Simon & Dyck (1977) showed this interpretation is roughly consistent with observations of FU Ori and V1057 Cyg.

The far-IR emission could potentially arise from local accretion energy or from dust heated by light from the central regions (“reprocessing”). The observations of V1057 Cyg’s decline from its 1971–1972 optical maximum strongly suggest that processing is responsible for the excess emission at *N* (10 μm) and *Q* (20 μm). The models we describe below indicate this emission arises in regions ~5–10 AU from the central star. The dynamical (free fall) time scale at this distance is roughly 10 yr, so accretion—particularly *viscous* disk accretion (see Pringle 1981)—cannot explain the decay on shorter time scales (Fig. 3). On the other hand, reprocessing of light from the central regions naturally explains why the 10–20 μm flux followed the optical light curves during the early portions of the decline from visual maximum (JD 2,441,000–2,443,000; see also Simon & Joyce 1988). At later times (JD 2,445,000–2,448,000), the 10–20 μm fluxes show a flatter decline than the visual. However, the peak of V1057 Cyg’s spectral energy distribution shifted from a wavelength of roughly 0.5 μm at visual maximum to roughly 1 μm during the optical decline, so the total system luminosity has decreased less than that indicated by the *V* light curve. We show in § 3.2 that the decline in the 10–20 μm flux is consistent with the drop in *bolometric* lumi-

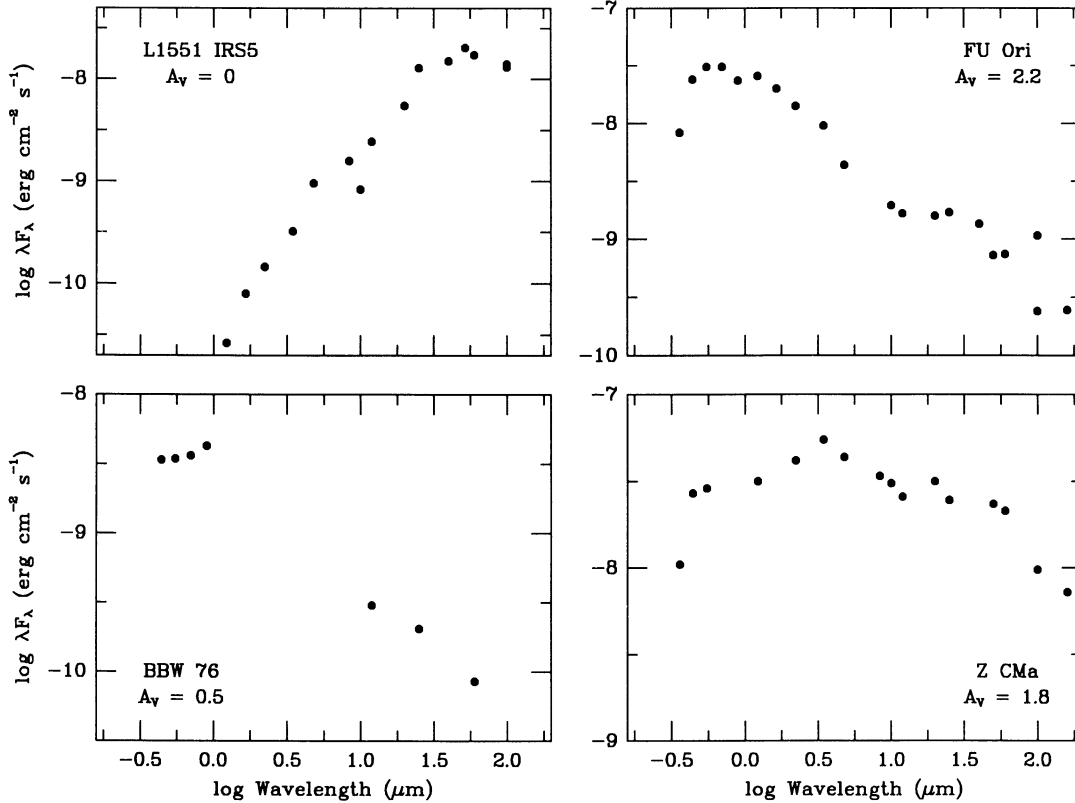


FIG. 2.—Spectral energy distributions for the FU Orionis objects L1551 IRS 5, FU Ori, BBW 76, and Z CMa. The data have been dereddened by the amounts shown in each panel. The fluxes have been compiled from Beichman & Harris (1981; L1551 IRS 5), Cohen (1980; Z CMa), Cohen & Schwartz (1983; L1551 IRS 5), Cohen et al. (1984; L1551 IRS 5), Eisloffel et al. (1990; BBW 76), Evans, Levreault, & Harvey (1986; Z CMa), Fridlund et al. (1980; L1551 IRS 5), Graham & Frogel (1985; FU Ori), Harvey & Wilking (1982; FU Ori), Lorenzetti, Saraceno, & Strafella (1983; Z CMa), Simon & Dyck (1977; Z CMa), Smith et al. (1982; FU Ori), and this paper.

nosity. For these reasons, we prefer a reprocessing model to explain the far-IR excess in V1057 Cyg.

The large far-IR excess emission in V1057 Cyg requires a substantial dust opacity in the envelope that is far in excess of the modest $A_V = 3.5$ derived from the optical spectral energy distribution (see the discussion of ALS). We are thus motivated to consider models in which the dust envelope is not spherically symmetric, but flattened, with low extinction along the line of sight.

3.1. Flared Disk Models

KHH noted additional far-IR emission in FU Orionis variables might be produced with steady accretion if dusty material in the outer portions of the disk absorbed and reradiated photons emitted by inner disk regions. Stellar radiation absorbed and reprocessed by a circumstellar disk has been discussed by several authors, including Friedjung (1985), Adams & Shu (1986), ALS, Kenyon & Hartmann (1987, hereafter KH), and Smak (1989). Here we consider *inner disk* emission absorbed and reprocessed by material in outer disk annuli. Our calculation is based on the geometry described in the Appendix of KH, where the height of the disk photosphere above the midplane, $H_d(R)$, increases with radius R :

$$H_d(R)/R_* = H_0(R/R_*)^z, \quad (1)$$

where R_* is the radius of the central star and $z > 0$. If $z = 0$, the disk is flat and a given annulus receives no radiation from other disk annuli.

We work in a cylindrical coordinate system, (ϖ, θ, z) , where ϖ is the cylindrical radius in units of the stellar radius, R_* . Let \hat{n} and \hat{n}_0 be the unit normals to the disk surface at two points, P and P_0 , where P_0 lies closer to the star than P . The flux absorbed by a unit area of the disk is

$$- (\hat{S} \cdot \hat{n})(\hat{S} \cdot \hat{n}_0) I(\varpi) \frac{2\varpi d\varpi d\theta}{l^2}, \quad (2)$$

where \hat{S} is the unit vector from P_0 to P , l is the distance from P_0 to P , and $I(\varpi)$ is the radiation intensity emitted at P_0 .

The disk radiates as a classical α -model (Shakura & Sunyaev 1973):

$$\pi I(\varpi) = \sigma T_A^4(\varpi) = \sigma T_*^4 \varpi^{-3} (1 - \sqrt{1/\varpi}), \quad (3)$$

where T_* is the disk's characteristic temperature,

$$T_* \approx 26,885 \text{ K} \left(\frac{M_*}{1 M_\odot} \right)^{1/4} \left(\frac{\dot{M}}{10^{-5} M_\odot \text{ yr}^{-1}} \right)^{1/4} \left(\frac{R_*}{R_\odot} \right)^{-3/4}. \quad (4)$$

The local “reprocessing temperature,” $T_R(R)$, is then

$$\left(\frac{T_R(R)}{T_*} \right)^4 = \frac{2}{\pi} \int_1^R \int_1^{\theta_{\max}(\varpi)} - \frac{(\hat{S} \cdot \hat{n})(\hat{S} \cdot \hat{n}_0)}{l^2} \left(1 - \sqrt{\frac{1}{\varpi}} \right) \frac{d\varpi d\theta}{\varpi^2}, \quad (5)$$

where θ_{\max} accounts for the occultation of the disk by the

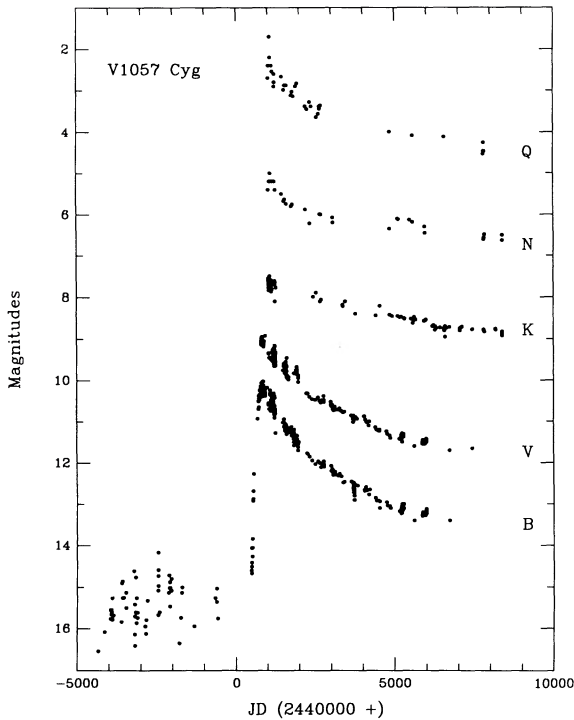


FIG. 3.—Optical and IR light curves for V1057 Cyg. The N and Q data have been displaced by +5 mag for this plot, while the K data have been displaced by +3 mag. The B and V points have been plotted as observed. The data have been compiled from Cohen & Woolf (1971), Mendoza (1971), Kiselev (1972), Rieke et al. (1972), Schwartz & Snow (1972), Simon et al. (1972), Gieseking (1973, 1974), Grasdalen (1973), Cohen (1973a, b, 1975), Landolt (1975, 1977), Mandel (1975), Simon (1975), Kolotilov (1977, 1990), Simon & Dyck (1977), Mould et al. (1978), Hopp, Kiehl, & Witzigmann (1979), Welin (1983), Kopatskaya (1984), Shaimieva & Shutiomova (1985), Kenyon et al. (1988), Simon & Joyce (1988), and this paper.

central star. The limits of the radial integral do not allow disk annuli with $\varpi > R$ to reprocess radiation; this approximation underestimates $T_R(R)$, but the error is negligible. We compute $T_A(R)$ for a specific set of accretion parameters, M_* , R_* , \dot{M} , and then determine $T_R(R)$ due to reprocessing. The disk temperature, T_d , is then calculated assuming blackbody radiators: $T_d^4 = T_A^4 + T_R^4$. We have not made any attempt to derive a “self-consistent” model in which the scale height of the disk is determined by the local disk temperature, T_d . Our previous analysis suggests that a self-consistent model probably results in a slightly flatter temperature distribution, and hence a larger far-IR excess, than the case we consider below (see KH).

Figure 4 presents temperature distributions for a standard flared disk model in which the exponent in equation (1) is $z = 9/8$ (KH). The solid line shows $T_d(R)$ for a classical α -model (see eq. [19]); this temperature distribution is also produced in a stellar reprocessing model when the scale height of the disk is zero everywhere (ALS). The remaining lines plot $T_d(R)$ for increasingly “fatter” disks as viewed from the disk midplane. The disk photosphere lies ~ 3 scale heights above the midplane when $H_0 = 0.1$.

Figure 5 displays several model energy distributions for flared reprocessing disks and compares them with observations of V1057 Cyg (*right panel*) and FU Ori (*left panel*). We assume disk annuli radiate as supergiant stars for $T_d > 3300$ K and as blackbodies for $T_d \leq 3300$ K; the disk is truncated when the local temperature falls below 50 K. The lack of disk annuli

with $T_d < 50$ K causes our spectral energy distributions to turn over for $\lambda > 60$ – $100 \mu\text{m}$. We also adopted models for FU Ori and V1057 Cyg developed by KHH: $T_* = 14,744$ K for FU Ori and $T_* = 13,495$ K for V1057 Cyg (see eq. [4]).

Energy distributions for modestly flared ($z = 9/8$) reprocessing disks begin to exhibit excesses over standard α -model disks for wavelengths exceeding 10 – $20 \mu\text{m}$ (Fig. 5). These excesses are small for $H_0 \lesssim 0.05$ but become substantial when $H_0 \sim 0.1$. The spectral energy distribution for $H_0 \sim 0.1$ exhibits a plateau from 10 to $100 \mu\text{m}$ that is roughly one order of magnitude below the peak in the energy distribution at $1 \mu\text{m}$.

The model energy distributions agree with the observations if $H_0 \sim 0.05$ for FU Ori and $H_0 \sim 0.20$ for V1057 Cyg. The height of the disk photosphere above the midplane in the FU Ori model is small, $H_d/R \sim 0.1$ at $R \sim 10$ AU, and is consistent with KH’s estimate for typical T Tauri stars. FU Ori shows no strong evidence for the $10 \mu\text{m}$ and $20 \mu\text{m}$ silicate emission features expected from an optically thin shell surrounding a bright central source, so an optically thick, flared disk model seems a reasonable explanation for the small far-IR excess observed in this system. This model can also account for the level of the 10 – $60 \mu\text{m}$ emission observed in V1057 Cyg; however, the flaring required is severe, $H_d/R \sim 0.4$ at $R \sim 10$ AU, and additional emission from optically thin dust is needed for the $10 \mu\text{m}$ and $20 \mu\text{m}$ emission lines observed near visual maximum (see Fig. 7). The structure of an extremely flared disk qualitatively resembles the optically thin, infalling envelope models described by ALS, and we consider similar models for the far-IR emission in the next section.

3.2. Infalling Dust Envelope Models

ALS noted a modest far-IR excess in FU Ori, above the prediction of steady disk models. They suggested this excess

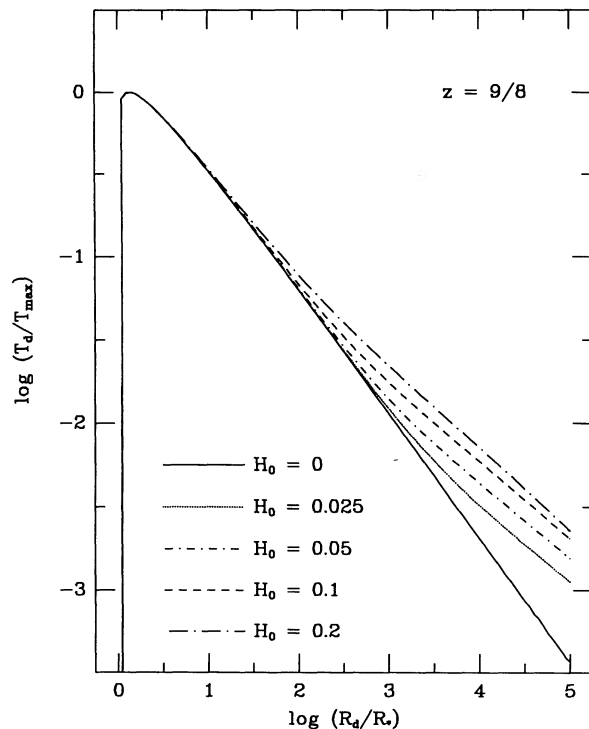


FIG. 4.—Radial temperature distributions for the flared reprocessing disk model described in the text.

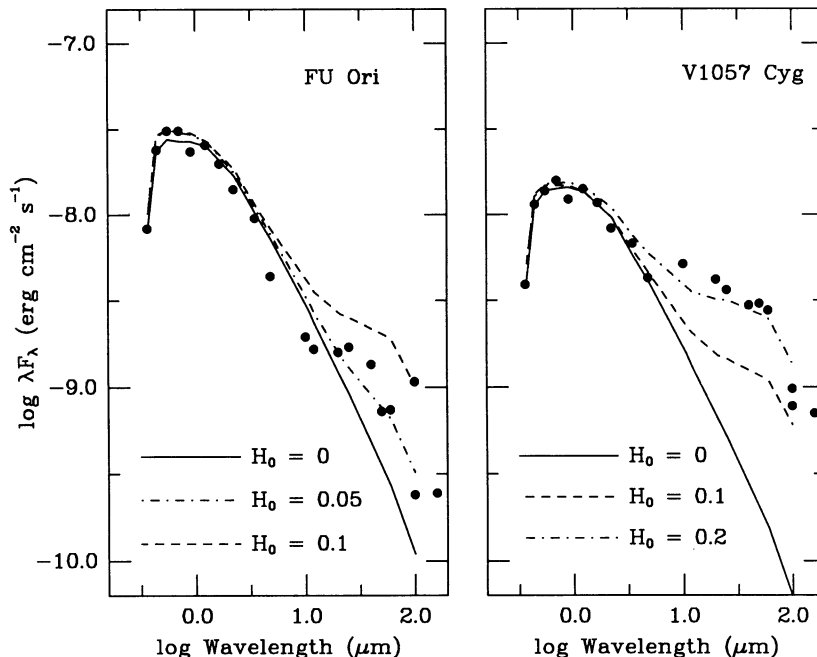


FIG. 5.—Spectral energy distributions of FU Ori (left panel) and V1057 Cyg (right panel) compared to models of flared reprocessing disks

emission arises in the remnant outer envelope of a molecular cloud core that reprocesses radiation from regions close to the central star. ALS adopted the observed visual extinction of FU Ori, $A_V \sim 2.5$, for the extinction through this remnant envelope and assumed that the envelope covered a small fraction, $f \sim 0.1$, of solid angle as seen from the central star to produce the correct far-infrared luminosity. ALS were forced to assume that the envelope has been “depleted” by a factor of 100 from its original isothermal sphere density structure to account for the spectral energy distribution of the far-IR excess.

The ALS model cannot explain the far-IR excess of V1057 Cyg if the extinction through the envelope, $A_V(\text{env})$, equals the observed line-of-sight visual extinction, $A_V(\text{los}) \sim 3.5$ (KHH). These models are very optically thin at far-IR wavelengths and produce modest amounts of far-IR emission comparable to that observed in FU Ori (see Figs. 2 and 5). However, the optical extinction to the central light source in V1057 Cyg may not be a good measure of the optical depth through the dusty envelope. Goodrich (1987) attempted to explain the ring-shaped reflection nebula around V1057 Cyg as the limb-brightened rim of a conical structure seen nearly pole-on. The notion that V1057 Cyg is observed at low inclination angle, i , is supported by the modest rotational velocity, $v \sin i$, measured for the disk (KHH). Thus, V1057 Cyg may be observed through a “hole” in the envelope, which could be produced by a bipolar outflow as conjectured by Shu, Adams, & Lizano (1987). We have therefore investigated models for the far-IR emission in which there is a hole in the dusty envelope along the line of sight.

The absence of observational constraints on the envelope’s geometry justifies a schematic approach. We follow the procedure outlined by ALS with small modifications to account for finite optical depth effects. Figure 6 shows a simple illustration of the model as viewed from the disk midplane. In the upper panel, material in the shaded envelope falls onto the

at an inner radius, r_0 . The Terebey, Shu, & Cassen (1984) calculation for a rotating, infalling envelope produces a velocity field that is essentially radial at large distances and departs from radial flow only close to the disk. The density distribution of this envelope is fairly isotropic in the absence of a wind (see Chevalier 1983), so we approximate the envelope as spherically symmetric, with inner radius r_0 , and a wind-driven polar hole (Fig. 6; lower panel). The hole subtends an angle, θ , from the polar axis and is axisymmetric, so the envelope covers a solid angle, $4\pi f = 4\pi \cos \theta$, as viewed from the central star. We depart from ALS by assuming that the envelope consists of freely falling dusty material, rather than the density distribution of a “depleted” isothermal sphere. The reasons for this choice will become evident later. Assuming steady state infall, the density distribution, ρ , is determined as a function of radial distance in spherical coordinates, r , by the equation

$$\rho = \frac{\dot{M}}{4\pi r^3 (2GM_*)^{1/2}}, \quad (6)$$

where $f\dot{M}$ is the total mass accretion rate of the envelope and M_* is the mass of the central star.

The inner radius of the envelope, r_0 , is related to the visual extinction through the envelope $A_V(\text{env})$ by

$$r_0 = \frac{k_V^2 \dot{M}^2}{8\pi^2 GM_* A_V^2(\text{env})}, \quad (7)$$

where k_V is the opacity per gram at V . We assume $A_V(\text{env})$ is not necessarily the observed visual extinction to the central object, $A_V(\text{los})$. We also assume the envelope is sufficiently optically thick at short wavelengths to absorb all of the incident light from the central object, so the luminosity of the envelope is related to the luminosity of the central source by $L(\text{env}) = fL_{\text{disk}}$.

For simplicity we assume the envelope is viewed along the polar axis and calculate the “apparent luminosity” at fre-

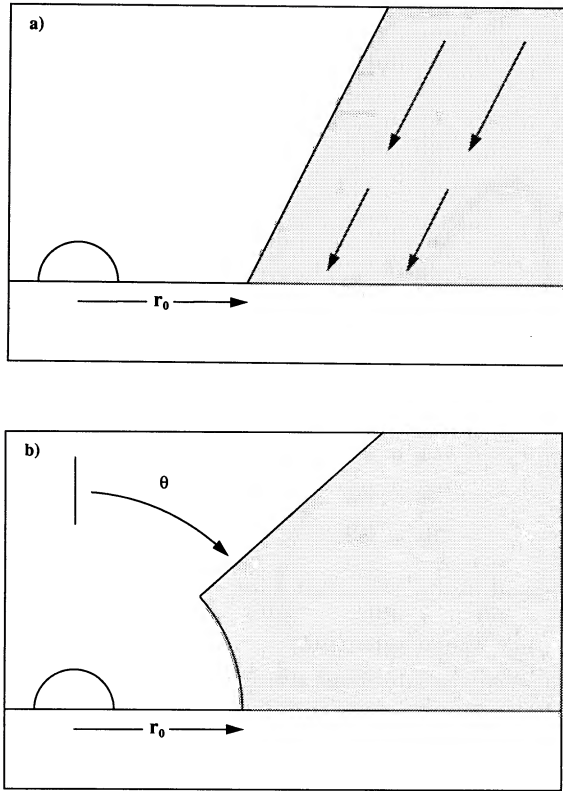


FIG. 6.—Infalling envelope model as viewed from the disk midplane. (a) Upper panel shows the envelope expected from a rotating, infalling cloud (see Terebey et al. (1984)). (b) Lower panel shows the spherically symmetric envelope modeled in the text.

quency ν ,

$$L_{\nu}(\text{app}) = \int_{r_0}^{r_{\text{max}}} 2\pi p dp \int_0^{\tau_{\nu}(\text{max})} B_{\nu}(p, \tau_{\nu}) e^{-\tau_{\nu}} d\tau_{\nu}, \quad (8)$$

where p is the perpendicular distance from the axis, B_{ν} is the Planck function, and the integrals are taken over the appropriate volume of the envelope. We also assume photons emitted into the disk by the upper envelope are not reprocessed by the disk but are absorbed or “lost,” and that photons from the lower half of the envelope are occulted from view by a large optically thick disk.

We chose an outer radius for the envelope, $r_{\text{max}} = 0.1$ pc, comparable to the sizes of dense molecular cloud cores (see, for example, Benson & Myres 1989). This radius contains a mass, $\sim 1 M_{\odot}$, close to our estimated mass for the central source, $M_{*} \sim 0.3\text{--}1.3 M_{\odot}$, for most cases of interest. However, most of the far-IR emission is produced in a much smaller volume with a radius of roughly 2000 AU and a mass of roughly $0.05 M_{\odot}$. This material has a free-fall time scale of $\sim 10^5$ yr, which is short compared to a typical pre-main-sequence lifetime of 10^6 yr (Cohen & Kuhl 1979).

We adopt a temperature distribution given by $T \propto r^{-0.33}$, which is appropriate for optically thin envelopes with the dust opacity law adopted by ALS, $k_{\nu} \propto \lambda^{-2}$ (see also Emerson 1988). Strictly speaking, the temperature distributions calculated in this way are valid only in the optically thin limit. However, the radial optical depths through the envelope in the models considered here are of order unity in the wavelength

range 5–50 μm , where most of the envelope’s radiation is emitted.

The temperature at r_0 is approximately

$$T_0 \sim \left[\frac{4\pi^3 (GM_{*})^2 L_{\text{acc}} A_V^3(\text{env})}{BM^4 \sigma k_V^3} \right]^{1/6} \quad (9)$$

where L_{acc} is the accretion luminosity of the inner disk. We use a Planck mean opacity, $k_p = BT^2$, where $B = 2.38 \times 10^{-4} \text{ cm}^2 \text{ g}^{-1} \text{ K}^{-2}$. Equation (9) is analogous to equation (27) of ALS, modified for $\rho \propto r^{-1.5}$ rather than $\rho \propto r^{-2}$. This expression for T_0 is an approximation to obtain the correct envelope luminosity for a central point source with a luminosity of L_{acc} and ignores the flat geometry of the inner disk. However, most of the disk radiation is emitted by annuli with radii small compared to r_0 , so this assumption introduces only a small uncertainty compared to other approximations in our spherically symmetric calculation. For cases of interest, equation (8) produces the correct envelope luminosity to within $\sim 30\%$.

In practice, we adjusted T_0 slightly to obtain the desired luminosity $fL_{\text{acc}} = \int L_{\nu}(\text{app}) d\nu$. We calculated the total envelope luminosity assuming that the emergent radiation is isotropic. This procedure is not strictly correct, because the modest optical depths through the envelope imply that the emergent flux is dependent upon the viewing angle. Given the approximate nature of the radiative transfer and the lack of constraints on f , we prefer to ignore these complications in the present study. Our approximations preserve the essential feature of the model, namely that the dust envelope fluxes remain a fixed fraction of the input luminosity.

We used the ALS opacity law (see also Adams & Shu 1986) except at 18 μm . The ALS curve has two peaks at 16 μm and 21 μm , whereas a peak at 18 μm appears to agree better with observations of red giants and other Galactic sources with significant circumstellar dust emission (see, for example, Jones & Merrill 1976; Draine & Lee 1984). The 18 μm observations of V1057 Cyg also require an 18 μm peak (see Fig. 7). We therefore increased the opacity at this wavelength to agree with the ratio of opacities at 10 μm and 18 μm suggested by Draine & Lee (1984).

Aside from the 10 μm and 18 μm silicate features, the ALS opacity law has a strong feature at 3.1 μm due to water ice. We do not predict the amount of 3 μm emission from our model, because the temperature structure near the envelope’s inner boundary—where most of the 3 μm emission would be produced—is very poorly treated. Moreover, thermal disk emission dominates the envelope emission at wavelengths less than 10 μm (see Fig. 7), so any ice emission produced by the envelope is not detectable. Ice absorption is not predicted by the model, because the line of sight to the central source does not intersect the envelope.

Figure 7 compares our model energy distributions with observations of V1057 Cyg at four epochs. The data have been corrected for interstellar reddening, $A_V(\text{los}) = 3.5$ (KHH), and each panel is labeled with the Julian Date of the observation and the total luminosity from 0.36 μm to 5 μm . This luminosity has been increased by roughly 10% near optical maximum (JD 2,441,000–2,441,220) to account for ultraviolet emission expected from an A-type photosphere. The luminosity correction for the G-type photosphere observed at later times is negligible, and ultraviolet spectra described by Kenyon et al. (1989) confirm that V1057 Cyg emits a very small fraction of its total luminosity at ultraviolet wavelengths for a standard

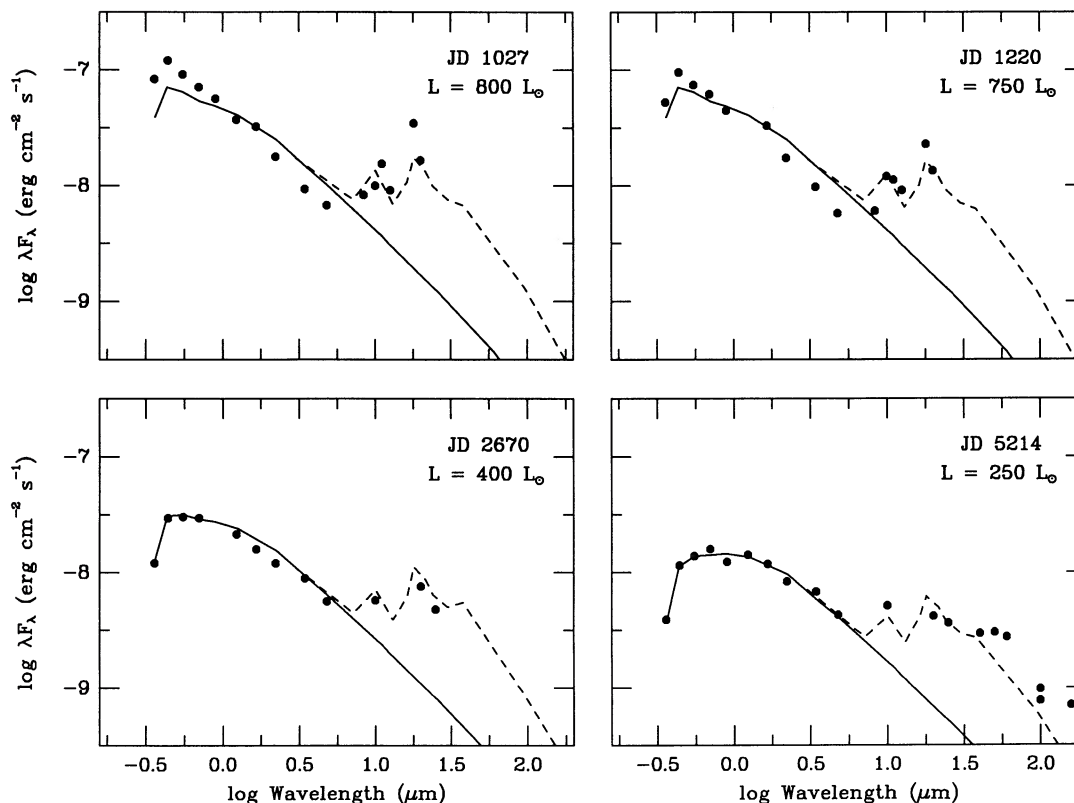


FIG. 7.—Comparison of observed spectral energy distributions of V1057 Cyg (from Fig. 4) with accretion disk models surrounded by an infalling envelope with $r_0 = 6$ AU and $\dot{M} = 4 \times 10^{-6} M_\odot \text{ yr}^{-1}$. The mean Julian Date (JD = 2,440,000 + JD listed) and the luminosity of the optical/near-IR source is listed in each panel. The solid line in each panel is the energy distribution of the steady accretion-disk model that produces the listed luminosities, while the dashed lines show the extra radiation produced by the infalling envelope.

reddening law and $A_V(\text{los}) = 3.5$. We have not tried to correct the luminosity for emission at wavelengths exceeding $5 \mu\text{m}$; if the slope of the far-IR continuum follows the near-IR slope, this correction is less than 10%.

The model energy distributions have two radiation sources: the accretion disk and the envelope. We adopted the steady disk model of KHH for JD 2,445,214 and increased the accretion rate at fixed inner disk radius to produce the appropriate optical/near-IR luminosity for earlier epochs. The observed energy distribution near visual maximum, dereddened by $A_V(\text{los}) = 3.5$, is slightly bluer than the model. The agreement between our model—shown as the solid line—and these early observations could be improved with a smaller reddening correction, $A_V(\text{los}) \sim 2.5$ – 2.7 , but this value for $A_V(\text{los})$ is not consistent with the optical spectral type and broad-band colors at later epochs (see KHH). The overall agreement at short wavelengths is fairly good when we consider that the steady disk assumption is not strictly appropriate near maximum light when the disk luminosity is evolving very rapidly. Similarly large departures from a steady state structure are observed in evolving very rapidly. Similarly large departures from a steady state structure are observed in time-dependent calculations of cataclysmic variable disks near maximum light (see, for example, Cannizzo & Kenyon 1987; Pringle, Verbunt, & Wade 1986).

The envelope models in Figure 7 are characterized by $f = 0.5$, $r_0 = 1 \times 10^{14}$ cm, and $\dot{M} = 4 \times 10^{-6} M_\odot \text{ yr}^{-1}$ (with $M_* = 1 M_\odot$). The inner radius of the dust envelope must be ~ 10 AU to produce a significant excess at $10 \mu\text{m}$, and this

material has a dynamical (free-fall) time of roughly 10 yr. The outburst of V1057 Cyg has already lasted 20 yr, so this material probably is not part of the original static envelope. It is more probable that the dust envelope is part of the infalling material that formed the disk, which is consistent with our assumption of $\rho \propto r^{-3/2}$ (for steady infall).

The visual extinction through the envelope is $A_V(\text{env}) = 50$, but the optical depth is small at wavelengths of 60 – $100 \mu\text{m}$. The spectral energy distribution is not changed appreciably if we remove the portion of the disk that occults the far side of the envelope. If the disk occultation is eliminated, $f = 0.25$ would produce the same far-IR luminosity.

The dust envelope model matches the time evolution of the emission at 10 – $20 \mu\text{m}$ reasonably well. The $18 \mu\text{m}$ observations near visual maximum are higher than our model predictions, which could be caused by observational errors in the $18 \mu\text{m}$ flux (see Fig. 3) or by our simple radiative transfer calculations. Our model also does not emit enough far-IR emission at JD 2,445,214. The decrease in fluxes beyond $30 \mu\text{m}$ occurs because the envelope becomes optically thin, and the emission drops rapidly as the dust opacity decreases. A more satisfactory model could be produced if the envelope opacity were increased. However, we are reluctant to increase the optical depths with our simple $T \propto r^{-1/3}$ approximation, because the use of this relation is already somewhat questionable when—as in our case—the envelope is not optically thin at short wavelengths. We suspect that $T \propto r^{-1/2}$ might be more appropriate for V1057 Cyg, when even larger optical depths would be required to reproduce the observed far-IR fluxes.

Despite these slight deficiencies of the model in reproducing the details of the observations, it is clear that the decline in 10–20 μm fluxes can be understood as a response to the *bolometric* heating of the envelope by the inner disk (see § 2).

An accurate treatment of the dust envelope radiation in V1057 Cyg requires a sophisticated radiative equilibrium calculation and a careful treatment of the envelope geometry, which is beyond the scope of this paper. The present crude models, however, serve to illustrate that the optical depth of this dust envelope must be much greater than indicated by the line-of-sight visual extinction.

4. DISCUSSION

Our analysis of V1057 Cyg suggests the far-IR emission is optical radiation absorbed and reprocessed by a dusty, opaque envelope. This conclusion is based on two main points: the far-IR and optical luminosity decline together, and the time scale for the far-IR decline—10 yr—is equal to the optical decline but is shorter than the disk's dynamical time scale. The envelope is optically thick— $A_V(\text{env}) \geq 50$ –100—and must cover $\sim 25\%$ – 50% of solid angle as viewed from the central star to account for the observed luminosity. This FU Orionis variable must be observed nearly pole-on to see radiation emitted by the inner disk (see also Weintraub et al. 1991), which is consistent with the low $v \sin i$ measured from optical spectra and the geometry of the large optical reflection nebula (KHH; Goodrich 1987).

If V1057 Cyg is typical of the FU Orionis class and FU Orionis variables are oriented randomly in the plane of the sky, then $\sim 50\%$ should be viewed *through the envelope* if the covering factor is $f \sim \frac{1}{2}$ in most systems. These objects should have $L_{\text{IR}}/L_{\text{opt}} \gg 1$, because nearly all of the optical radiation along the line of sight is absorbed. Observations of L1551 IRS 5 and V346 Nor are consistent with this picture, and V1735 Cyg has the large optical extinction expected for a source viewed through the “edge” of the envelope. The strong 3.1 μm water ice absorption feature observed in L1551 IRS 5 is characteristic of young stars with $A_V(\text{los}) \gtrsim 20$ (ALS; Sato et al. 1990), while water ice absorption in V1735 Cyg suggests $A_V(\text{los}) \sim 10$ (Sato et al. 1990). A fourth system—Z CMa—may have a similar geometry, because its spectral energy distribution resembles V346 Nor. Thus, three to four out of eight FU Orionis variables appear to be viewed through a very opaque, dusty envelope, which is crudely consistent with our inferred covering factor of $f \sim \frac{1}{2}$.

The idea that L1551 IRS 5 is viewed through an infalling envelope is supported by the calculations of ALS, who showed that its IR spectral energy distribution is consistent with their protostellar models (see, however, Butner et al. 1991). ALS estimated a mass infall rate of $\sim 7 \times 10^{-6} M_{\odot} \text{ yr}^{-1}$ for IRS 5, which is comparable to our estimate for V1057 Cyg.

Weintraub et al. (1991) have reached similar conclusions concerning the flattened geometry of dusty material surrounding FU Orionis variables. Their estimates of the dust mass needed to produce the observed submillimeter fluxes are comparable to that contained in our infalling envelope for V1057 Cyg— $M_{\text{submm}} \sim 0.1 M_{\odot}$ versus $M_{\text{env}} \gtrsim 0.05 M_{\odot}$ for $f = \frac{1}{2}$ —and their measured sized for V1735 Cyg and V346 Nor are also close to our adopted outer radius for the envelope— $R_{\text{submm}} \sim 10^4 \text{ AU}$ versus $R_{\text{env}} \sim 2 \times 10^4 \text{ AU}$. We differ from Weintraub et al. (1991) in associating the far-IR and submillimeter continuum flux with envelope emission (as in ALS and Butner et al. 1991), rather than disk emission. As we

stated above, the time evolution of the spectral energy distribution of V1057 Cyg is too rapid to associate the observed far-IR flux with intrinsic disk emission. Reprocessing of inner disk emission by dusty material in a flared disk can reproduce the observed far-IR spectral energy distributions of FU Orionis variables, but the disk must have a very large scale height to account for the large far-IR excesses observed in V1057 Cyg and V1515 Cyg. We prefer to associate this material with an infalling envelope.

The picture of FU Orionis variables as accretion disks surrounded by optically thick infalling envelopes of gas and dust also provides a natural explanation of multiple FU Orionis eruptions. Although the event statistics are crude, the detection of eight FU Orionis eruptions in the last 100 yr requires *each* low-mass main-sequence star within $\sim 1 \text{ kpc}$ of the Sun to undergo ~ 10 outbursts during its lifetime as a pre-main-sequence star (Herbig 1977; Hartmann & Kenyon 1985). If the central star accretes $\sim 0.01 M_{\odot}$ from a 0.1 – $0.2 M_{\odot}$ circumstellar disk during a typical FU Orionis event, the disk can be replenished in 10^3 – 10^4 yr for an infall rate of 1 – $10 \times 10^{-6} M_{\odot} \text{ yr}^{-1}$. We emphasize that the physical mechanism responsible for FU Orionis eruptions have not been identified, although thermal instabilities in the inner disk seem promising (see Clarke, Lin, & Pringle 1990).

Reipurth (1989b) has commented that mass outflows from several young stars appear episodic, as might be expected if winds from FU Orionis disks are responsible for most material ejected by young stars (see also Hartmann et al. 1991). In particular, multiple ejections have been invoked for the large line widths in the Herbig-Haro objects in HH 32 and L1551 (see Hartigan, Mundt, & Stocke 1986; Stocke et al. 1988), as well as the shape and velocity characteristics of HH 47 A (Hartigan, Raymond, & Meaburn 1990). Reipurth (1989a) has suggested two distinct ejections provide the best explanation for the twin bow shocks in HH 111. The interval between the two ejections is estimated to be $\sim 2000 \text{ yr}$ for HH 47 A (Hartigan et al. 1990) and 500 – 1000 yr for HH 111 (Reipurth 1989a). These time scales are comparable to the time estimated above for replenishing the disk after an FU Orionis eruption.

The large envelope extinctions of FU Orionis variables suggest these objects are relatively young. Our estimated infall rate of $5 \times 10^{-6} M_{\odot} \text{ yr}^{-1}$ for V1057 Cyg is comparable to the rates expected for cold cloud cores in the Taurus and Ophiuchus clouds (see Adams & Shu 1986), and similar infall rates of 1 – $10 \times 10^{-6} M_{\odot} \text{ yr}^{-1}$ have been estimated from observations of embedded sources in these clouds (Myers et al. 1987; Wilking, Lada, & Young 1989). The ages for embedded sources in the Taurus and Ophiuchus clouds are usually estimated at 1 – $3 \times 10^5 \text{ yr}$ (Myers et al. 1987; Wilking, Lada, & Young 1989; Kenyon et al. 1990), and our results suggest V1057 Cyg and other FU Orionis variables with large far-IR luminosities have similar ages (see also Weintraub et al. 1991). FU Ori and BBW 76 may be somewhat older than this estimate, because their far-IR luminosities are fairly modest.

The far-IR excess emission of V1057 Cyg, which we attribute to reprocessing of light emitted in the inner disk, is relatively constant in λF_{λ} from about 10 to $60 \mu\text{m}$. However, flat far-IR spectral energy distributions of other young stars have been attributed to accretion processes (ALS; Adams, Ruden, & Shu 1989). If the IR excess emission of these objects is really due to reprocessing, their IR variations should closely follow the optical light, just as in V1057 Cyg. Monitoring of other young stellar objects at optical and IR wavelengths may prove very useful in distinguishing between reprocessing and accretion.

We thank the staffs of the Infrared Telescope Facility, Multiple Mirror Telescope Observatory, and National Optical Astronomical Observatories for assistance with the observations reported in this paper, B. Soifer and IPAC for processing the *IRAS* data, and George Nassiopoulos for creating Figure 6. S. Austin, D. Backman, M. Gomez, P. Hartigan, and B. Whitney helped us acquire IR photometry at various sites.

We also acknowledge useful comments and suggestions from F. Adams, G. Fuller, P. Hartigan, C. Lada, T. Mouschovias, B. Whitney, and an anonymous referee. This research was supported in part by National Aeronautics and Space Administration grant NAGW-2306 and the Scholarly Studies Program of the Smithsonian Institution.

REFERENCES

- Adams, F. C., & Shu, F. H. 1986, *ApJ*, 308, 836
 Adams, F. C., Lada, C. J., & Shu, F. H. 1987, *ApJ*, 308, 788 (ALS)
 Adams, F. C., Ruden, S. P., & Shu, F. H. 1989, *ApJ*, 347, 959
 Beichman, C., & Harris, S. 1981, *ApJ*, 245, 589
 Benson, P. J., & Myers, P. C. 1989, *ApJS*, 71, 89
 Butner, H. M., Evans, N. J., II, Lester, D. F., Levreault, R. M., & Strom, S. E. 1991, *ApJ*, 376, 636
 Cannizzo, J. K., & Kenyon, S. J. 1987, *ApJ*, 320, 319
 Carr, J. S., Harvey, P. M., & Lester, D. F. 1987, *ApJ*, 321, L71
 Chevalier, R. A. 1983, *ApJ*, 268, 753
 Clarke, C. J., Lin, D. N. C., & Pringle, J. E. 1990, *MNRAS*, 242, 439
 Cohen, M. 1973a, *MNRAS*, 161, 85
 ———. 1973b, *MNRAS*, 161, 105
 ———. 1975, *MNRAS*, 173, 279
 ———. 1980b, *MNRAS*, 191, 499
 Cohen, M., Harvey, P. M., Schwartz, R. D., & Wilking, B. A. 1984, *ApJ*, 278, 671
 Cohen, M., & Kuhl, L. V. 1979, *ApJS*, 41, 743
 Cohen, M., & Schwartz, R. D. 1983, *ApJ*, 265, 877
 Cohen, M., & Woolf, N. J. 1971, *ApJ*, 169, 543
 Draine, B. T., & Lee, H. M. 1984, *ApJ*, 285, 89
 Eisloffel, J., Hessman, F. V., & Mundt, R. 1990, *A&A*, 232, 70
 Elias, J. H. 1978, *ApJ*, 223, 859
 Elias, J. H., Frogel, J. A., Matthews, K., & Neugebauer, G. 1982, *AJ*, 87, 1029
 Emerson, J. P. 1988, in *Formation and Evolution of Low Mass Stars*, ed. A. K. Dupree & M. V. T. V. Lago (Dordrecht: Kluwer), 21
 Evans, N. J., II, Levreault, R. M., & Harvey, P. M. 1986, *ApJ*, 301, 894
 Fridlund, C. V. M., Nordh, H. L., van Duinen, R. J., Aalders, J. W. G., & Sargent, A. I. 1980, *A&A*, 91, L1
 Friedjung, M. 1985, *A&A*, 146, 366
 Giesekeing, F. 1973, *Inf. Bull. Var. Stars*, No. 806
 ———. 1974, *A&A*, 31, 117
 Goodrich, R. 1987, *PASP*, 99, 116
 Graham, J. A., & Frogel, J. A. 1985, *ApJ*, 289, 331
 Grasdalen, G. L. 1973, *ApJ*, 182, 781
 Hartigan, P., Mundt, R., & Stocke, J. 1986, *AJ*, 91, 1357
 Hartigan, P., Raymond, J., & Meaburn, J. 1990, *ApJ*, 362, 624
 Hartmann, L. 1991, in *Physics of Star Formation and Early Stellar Evolution*, ed. C. J. Lada (NATO Adv. Study Inst.), in press
 Hartmann, L., & Kenyon, S. J. 1985, *ApJ*, 299, 462
 ———. 1987a, *ApJ*, 312, 243
 ———. 1987b, *ApJ*, 322, 393
 ———. 1991, in *IAU Colloq. 129, Structure and Emission Properties of Accretion Disks*, ed. S. Collin-Souffrin (Dordrecht: Kluwer), in press
 Hartmann, L., Kenyon, S. J., & Hartigan, P. 1991, in *Protostars and Planets III*, in press
 Hartmann, L., Kenyon, S. J., Hewett, R., Edwards, S., Strom, K. M., Strom, S. E., & Stauffer, J. R. 1989, *ApJ*, 338, 1001
 Harvey, P. M., & Wilking, B. A. 1982, *PASP*, 94, 285
 Herbig, G. H. 1977, *ApJ*, 217, 693
 Herbig, G. H. 1989, in *ESO Workshop on Low-Mass Star Formation and Pre-Main Sequence Objects*, ed. B. Reipurth (Garching: ESO), 233
 Hopp, U., Kiehl, M., & Witzigmann, S. 1979, *Inf. Bull. Var. Stars*, No. 1637
 Jones, T. W., & Merrill, M. K. 1976, *ApJ*, 209, 509
 Kenyon, S. J. 1988, *AJ*, 96, 337
 Kenyon, S. J., & Hartmann, L. 1987, *ApJ*, 323, 714 (KH)
 Kenyon, S. J., Hartmann, L., & Hewett, R. 1988, *ApJ*, 325, 231 (KHH)
 Kenyon, S. J., Hartmann, L., Imhoff, C. L., & Cassatella, A. 1989, *ApJ*, 344, 925
 Kenyon, S. J., Hartmann, L., Strom, K. M., & Strom, S. E. 1990, *AJ*, 99, 869
 Kenyon, S. J., Hartmann, L., & Kolotilov, E. A. 1991, *PASP*, submitted
 Kiselev, N. N. 1972, *Astron. Tsirk.*, No. 742
 Kolotilov, E. A. 1977, *Astron. Tsirk.*, No. 955
 ———. 1990, *Pis'ma Astron. Zh.*, 16, 24
 Kopatskaya, E. N. 1984, *Astrofizika*, 20, 275
 Landolt, A. U. 1975, *PASP*, 87, 379
 ———. 1977, *PASP*, 89, 704
 Lorenzetti, D., Saraceno, P., & Strafella, F. 1983, *ApJ*, 264, 554
 Mandel, O. E. 1975, *Perem. Zvezdy*, 20, 123
 Mendoza, E. E. V. 1971, *ApJ*, 169, L117
 Mould, J. R., Hall, D. N. B., Ridgway, S. T., Hintzen, P., & Aaronson, M. 1978, *ApJ*, 222, L123
 Mundt, R., Stocke, J., Strom, S., Strom, K., & Anderson, E. 1985, *ApJ*, 297, L41
 Myres, P. C., Fuller, G. A., Mathieu, R. D., Beichman, C. A., Benson, P. J., & Schild, R. E. 1987, *ApJ*, 319, 340
 Pringle, J. E. 1981, *ARA&A*, 19, 137
 Pringle, J. E., Verbunt, F., & Wade, R. A. 1986, *MNRAS*, 221, 169
 Reipurth, B. 1985, in *ESO Workshop on Low-Mass Star Formation and Pre-Main Sequence Objects*, ed. B. Reipurth (Garching: ESO), 249
 ———. 1989a, *Nature*, 340, 42
 ———. 1989b, in *ESO Workshop on Low-Mass Star Formation and Pre-Main Sequence Objects*, ed. B. Reipurth (Garching: ESO), 247
 ———. 1991, in *IAU Symposium 137, Flare Stars in Star Clusters, Associations, and the Solar Vicinity* (Dordrecht: Kluwer), in press
 Rieke, G., Lee, T., & Coyne, G. S. J. 1972, *PASP*, 84, 37
 Rodriguez, L. F., Hartmann, L. W., & Chavira, E. 1990, *PASP*, 102, 1413
 Sato, S., Nagata, T., Tanaka, M., & Yamoto, T. 1990, *ApJ*, 359, 192
 Savage, B. D., & Mathis, J. S. 1979, *ARA&A*, 17, 73
 Schild, R. 1977, *AJ*, 82, 337
 Schwartz, R. D., & Snow, T. P., Jr. 1972, *ApJ*, 177, L85
 Shaimieva, A. F., & Shutiomova, N. A. 1985, *Perem. Zvezdy*, 22, 172
 Shakura, N. I., & Sunyaev, R. A. 1973, *A&A*, 24, 337
 Shu, F. H., Adams, F. C., & Lizano, S. 1987, *ARA&A*, 25, 23
 Simon, T. 1975, *PASP*, 87, 317
 Simon, T., & Dyck, H. M. 1977, *AJ*, 82, 725
 Simon, T., & Joyce, R. R. 1988, *PASP*, 100, 1549
 Simon, T., Morrison, N. D., Wolf, S. C., & Morrison, D. 1972, *A&A*, 20, 99
 Smak, J. 1989, *Acta Astron.*, 39, 201
 Smith, H. A., Thronson, H. A., Jr., Lada, C. J., Harper, D. A., Loewenstein, R. F., & Smith, J. 1982, *ApJ*, 258, 170
 Staude, H. J., & Neckel, Th. 1991, *A&A*, in press
 Stocke, J. T., Hartigan, P. M., Strom, S. E., Strom, K. M., Anderson, E. R., Hartmann, L. W., & Kenyon, S. J. 1988, *ApJS*, 68, 229
 Terebey, S., Shu, F. H., & Cassen, P. 1984, *ApJ*, 286, 529
 Weintraub, D. A., Sandell, G., & Duncan, W. D. 1989, *ApJ*, 340, L69
 ———. 1991, *ApJ*, 382, 270
 Welin, G. 1983, *Inf. Bull. Var. Stars*, No. 2423
 Wilking, B. A., Lada, C. J., & Young, E. T. 1989, *ApJ*, 340, 823